Available online at: http://brsj.cepsbasra.edu.iq

ISSN –1817 –2695

Received 9-1-2018, Accepted 13-6-2018

Annealing Temperature Dependent Structural, Optical and Electrical Properties of Thermally Deposited CdSe Thin Films

Mohammad M. Ali

Department of Physics, College of Science, University of Basrah, Basrah, Iraq
Email: moh7077ali@gmail.com

Abstract

CdSe thin films have been deposited on suitably cleaned glass substrates by thermal evaporation method. The pressure during evaporation was maintained at 10^{-6} to 10^{-5} Torr. The samples are annealed in vacuum for 2h at various temperatures and characterized by structural, optical and electrical properties. The crystal structure and lattice parameter of these films were determined from X-ray diffractograms. It was observed that the films have a polycrystalline hexagonal (wurtzite) structure with preferred orientation along (002) plane. The crystallite size, dislocation density and micro strain were calculated by considering high intense diffraction peaks of the as-deposited and annealed films. It was found that the average size of the crystallites increases and the average dislocation density decreases with increasing annealing temperature. Absorption and transmittance spectra of these thin films were studied using UV-visible double beam spectrophotometer in the wavelength range of 300 – 1100 nm. The energy band gaps have been determined using absorption spectra. The values of the optical band gap energy, E_g, decreased from 2.37 – 2.08 eV with increasing the annealed temperature. Dependence of optical band gap on crystallite size has also been studied. The electrical resistivity and activation energy of CdSe thin films are calculated by two probe resistivity measurements. The decrease in dc resistivity with increase the grain size was also noted.

Keywords: Cadmium selenide, Thermal deposition, Annealing temperature, XRD, Crystallite size.

1. Introduction

Semiconducting thin film technologies are used for large area productions, minimizing the production costs. Now-a-days semiconducting nanocrystalline materials are used to convert solar energy into electricity. In nano materials the quantum dots increase the efficiency of solar power conversion through multiexcitons generation [1]. The semiconductor nanoparticles have properties

between molecules and bulk solids and their physicochemical properties are found to be strongly size dependent [2,3-8]. It is well known that the nanoscale systems show interesting physical properties, for example, increasing of the semiconductor band gap due to electron confinement [9-15]. Due to the effect of the spacing in the energy levels, the value of the energy gap is increased by decreasing nanocrystalline size [16-18]. At such crystalline dimensions, the photogenerated electron hole pairs are spatially confined [19], due to the large surface to volume ratio. The II-VI group compound semiconductors, due to their direct and large band gap, attract intense interest from both fundamental view point and the promising applications in electronic, optoelectronic, and photo-voltaic devices [20]. Cadmium selenide is one of the well-known of this group binary compounds as important material because of its containing active regions which can be used to produce light emission. The spectral range (460-530) nm and suitable band gap (1.74 eV) [21], can be used for optoelectronic devices such as solar cells[22], (PEC) cells [23] and light emitting diodes …etc. For the preparation of CdSe thin films, different methods have been used and reported in literature [24].

The structural parameters such as lattice constant, grain size, etc. are dependent on the deposition conditions. The structure of CdSe thin films is dependent on the rate of deposition, substrate temperature, vacuum conditions, film thickness, etc. In this paper, CdSe thin films were deposited by thermal evaporation method and the results have been analyzed and presented.

2. Experimental part

2.1. Substrate cleaning

The substrate cleaning is very important in the deposition of thin films. The properties of such a deposited film depends on the cleanliness of the substrate surface on which the film is deposited. Contamination on this surface can result in reduced adhesion of the film to the substrate, more rapid degradation of the film after deposition, greater contact resistance for electrically conducting films, and poor optical qualities for optical films. Even with careful handling, surface contamination in the form of adsorbed water vapor and a variety of hydrocarbons results from exposure to the laboratory atmosphere prior to deposition. This exposure can also cause the formation of native oxide layers on reactive substrate materials [25]. To remove this surface contamination, it is necessary to clean the substrate surface. Microslide glasses of dimensions of (75 mm x 25 mm x 1 mm) were used as substrates. Before deposition, the glass substrates were cleaned first by a mild soap solution, then degreased with acetone (99.5%), etched with 5% HCl for 24 hours and ultrasonically for 10 min, first in acetone and then in water: ethanol (1:1) solution and then rinsed with double distilled water.

2.2. Preparation of CdSe thin films

Thin films of CdSe that have thickness around 560 nm were deposited on chemically and ultrasonically cleaned glass substrates with the help of vacuum coating unit at room temperature for substrates. The CdSe film thickness was measured with commonly used weight difference method by using a sensitive microbalance. A clean evaporation source molybdenum boat was fixed in the filament holder inside the chamber. Stoichiometric CdSe powder has purity around 5N was placed in a molybdenum boat. When 10^{-6} Torr vacuum was attained in vacuum chamber by the combination of rotary and diffusion pump, the heater connected to the evaporation source

was switched on which in turn slowly heated the source of CdSe to temperatures grater then melting point. This allowed the evaporation of CdSe material. After finishing the deposition of all the samples, the CdSe thin films were subjected to an annealed at 200 ^{o}C, 300 ^{o}C and 400 ^{o}C, in vacuum for almost two hours. Annealed which is performed by a tubular furnace, afterwards the sample was allowed to cool down naturally. The aim of this post-deposition procedure is to improve the structural, morphological and chemical quality of the films.

2.3. Characterizations

The structure evolution of the as-deposited CdSe and annealed thin films was examined by high-resolution X-ray diffraction (HR-XRD) using X'pert pro MRD diffractometer (PANalytical company) system equipped with Cu-Kα radiation wavelength (λ= 0.15406 nm) in the range from 20^{o} to 80^{o}. The optical characteristics were studied at room temperature for CdSe using HeλIOS α UV-Visible spectrophotometer (ThermoSpectronic, England) at wavelengths ranging from 300 to 1100 nm.

3. Results and discussion

3.1. Structural analysis of CdSe thin films: X-ray diffraction

The crystallite size, structural phase, dislocation density (δ) and micro strain (ε) of the CdSe thin films have been determined using XRD measurements. Cadmium selenide can be formed having the hexagonal (wurtzite type) structure or the cubic (zinc-blende type) structure [26]. Figure 1 shows the XRD pattern of as-deposited and annealed CdSe thin films at different temperatures. The X-ray diffraction patterns indicate that the prepared films are polycrystalline and have a hexagonal (wurtzite) structure. The films are highly oriented toward (002) planes. There are three dominant diffraction peaks: (002), (101) and (103). The d-values for peaks in XRD patterns were calculated and have been given in Table-1 along with the standard JCPDS data [27]. It is good agreement between the calculated and the standard d-values for the hexagonal structure. Since, the thickness of the films was not sufficiently enough, the intensity of other peaks is almost negligible. The lattice parameters (a and c) of hexagonal phase of as-deposited and annealed thin films were calculated using Eq.(1) [28]:

$$\frac{1}{d^2} = \frac{4}{3}\frac{(h^2+hk+k^2)}{a^2} + \frac{l^2}{c^2} \qquad (1)$$

The calculated values are tabulated in Table 1. These values are in good agreement with the desired one as well as the reported data [27,29].

The crystallite size, dislocation density and micro strain were calculated by considering high intense diffraction peaks of the as-deposited and annealed films using Eqs.(2-4) and the values are listed in Table 1. Debye – Scherrer's formula [28]

$$D = \frac{0.9\lambda}{\beta\cos\theta} \qquad (2)$$

Where D is the crystallite size, λ is the wavelength of the X-ray source, β is the full width at half maximum value and θ is the Bragg's angle. The dislocation is imperfection in the crystal which is created during growth of the thin film.

The dislocation density (δ) was calculated from the crystallite size of the samples using Williamson and Smallman's formula [30]:

$$\delta = \frac{1}{D^2} \quad (3)$$

It was found that the average size of the crystallites increases and the average dislocation density decreases with increasing annealing temperature.

Figure (2) shows variation of crystallite size from 39-82 nm with annealing temperatures, which shows that the crystallinity of CdSe increases with annealing temperature.

The strain in thin film is defined as the disarrangement of lattice created during their deposition and depends upon the deposition parameters. The micro strain (ε) is obtained by using the relation:

$$\varepsilon = (\beta \cot\theta)/2 \quad (4)$$

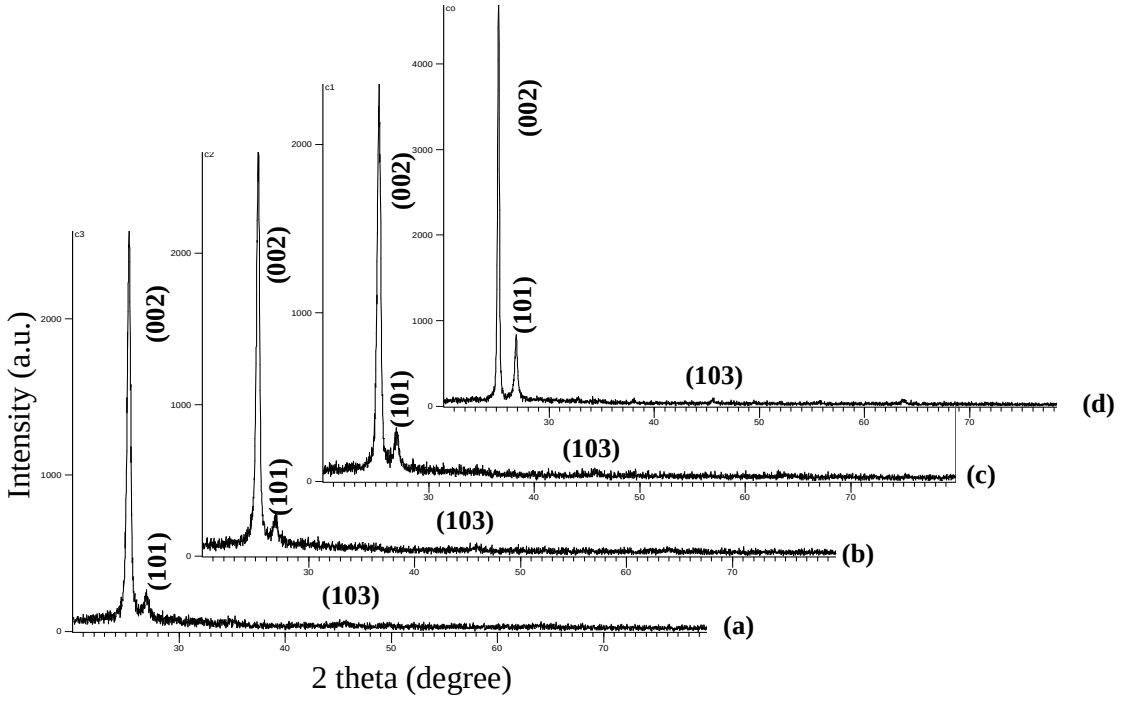

Fig. 1 XRD patterns of CdSe thin films (a) as-deposited and annealed at (b) 473 K, (c) 573 K and (d) 673 K.

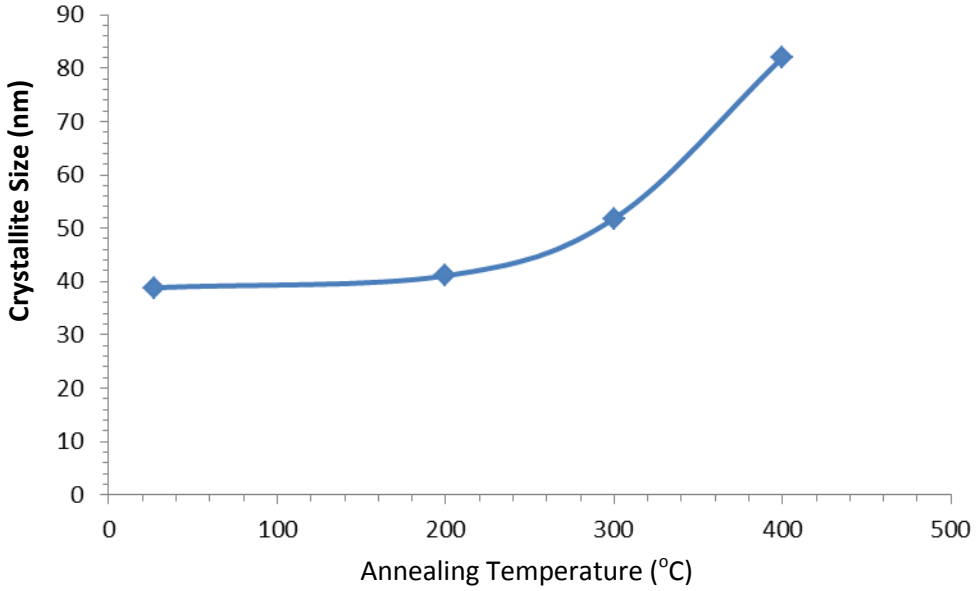

Fig. 2 Variation of crystallite size with annealing temperature of CdSe thin films.

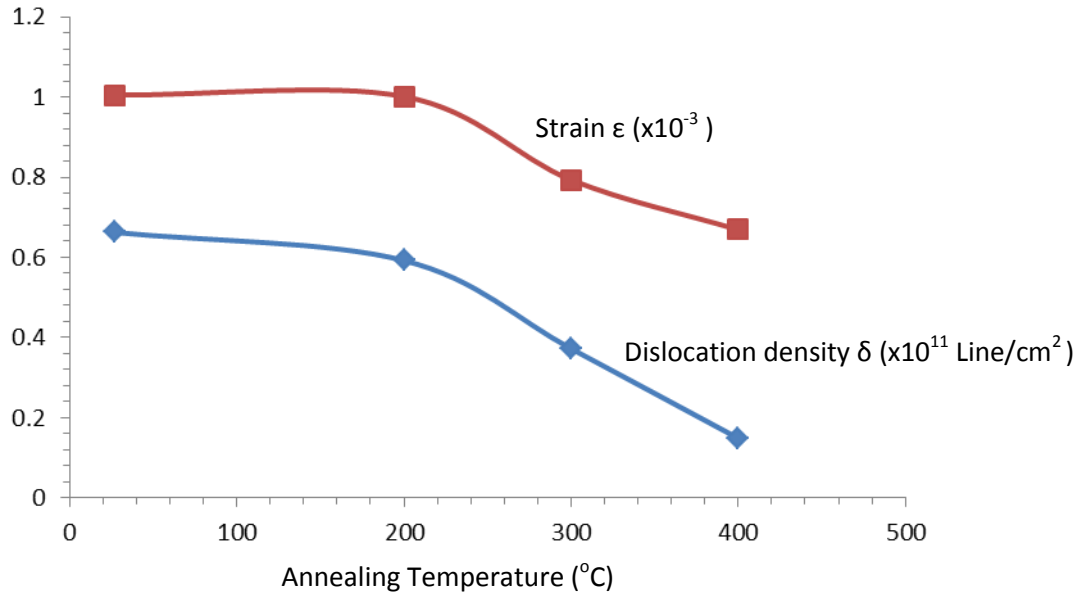

Fig. 3 Shows the variation of dislocation density and strain with annealing temperature of CdSe thin films.

Table 1: structural parameters of as-deposited and annealed CdSe thin films at different temperatures.

Thin films	2θ °		(hkl)	d-spacing(Å)		lattice parameters(Å)						crystallite size nm (Aver.)	δ x0^{11} Line/cm^2 (Aver.)	ε x10^{-3}
	Stan.	Obse.		Stan.	Obse.	Stan.		Ref. [29]		Obse.				
						a	c	a	c	a	c			
as-deposited	25.41	25.2948	(002)	3.5125	3.5210	4.311	7.025	----	----	4.326	7.042	39	0.662	1.0048
	26.76	26.9575	(101)	3.2929	3.3075									
annealed at 200 °C	25.58	25.3561	(002)	-----	3.5097	4.295	7.007	4.303	7.018	4.310	7.019	41	0.592	1.0012
	27.15	27.0341	(101)	-----	3.2956									
annealed at 300 °C	25.39	25.2975	(002)	-----	3.5115	4.304	7.020	4.310	7.029	4.327	7.023	52	0.372	0.7932
	27.11	26.9676	(101)	-----	3.3063									
annealed at 400 °C	25.41	25.1931	(002)	-----	3.5350	----	----	4.298	7.011	4.338	7.070	82	0.148	0.6687
	27.12	26.8703	(101)	-----	3.3180									

3.2.Optical properties

Figure 4 shows the variation of optical absorption and transmittance spectrum as a function to the wavelengths for as-deposited and annealed CdSe thin films. The results of these investigations have been used for the

calculations of absorption coefficients and other parameters. From the optical transmittance spectra, it is observed that the transmittance of the annealed CdSe thin films gets reduced compared to the film as-deposited at room temperature. While, it is apparent that the absorption spectra of annealed films have high optical absorption compared to those of as-deposited CdSe. These decreases in optical transmittance and increases in optical absorption spectra, it may be due to increase in crystallite size, the decrease in the number of defects, the change in lattice parameters and change in color from red-orange to dark brown.

The absorption coefficient α can be calculated by using the following relationship [31]:

$$\alpha = 2.303\frac{A}{t} \qquad (5)$$

Where t is the film thickness and A is the absorption. The absorption coefficient was found greater than 10^4 cm^{-1}, suggesting that CdSe has a direct band gap that increases sharply below a certain wavelength [32].

The fundamental absorption, which corresponds to the transition from the valence band to the conduction band, can be used to estimate the band gap of the semiconductor material. The relation between absorption coefficient α, and the incident photon energy hν, can be written as [33]:

$$\alpha = \frac{A(h\nu - E_g)^n}{h\nu} \qquad (6)$$

Where A is a constant, hν is the photon energy, E_g is the band gap and the parameter n depends on the type of electronic transition. The parameter n in the equation 6 can have values 1/2, 2, 3/2 and 3 for allowed direct, allowed indirect, forbidden direct and forbidden indirect transitions, respectively. The tangent drawn at absorption edge was extrapolated to energy axis i.e. zero absorption and the intercept value gives the optical band gap [34]. The band gaps (E_g) values for as-deposited and annealed hexagonal CdSe thin films were reported in Table 2 (see Figure 5(i)). The optical band gap values of the annealed CdSe thin films are higher than the value of the optical band gap of bulk CdSe (1.7 eV), this difference in band gap may be attributed to quantum-size effect [35].

As the annealing temperature was increased, the crystallite size of CdSe films was increased resulting in to decrease in band gap. Therefore, annealing the films, exhibits strong red shift in their optical spectra due to localization of charges in individual nanocrystals. Annealing of the films caused a gradual shift of the film spectra to that characteristic of bulk CdSe, due to sintering of the nanocrystallites into effectively larger crystallites. This agrees with the results reported earlier in the literature [36-39].

Figure (5(ii)) shows the variation of band gap E_g versus crystallite size of CdSe thin films.

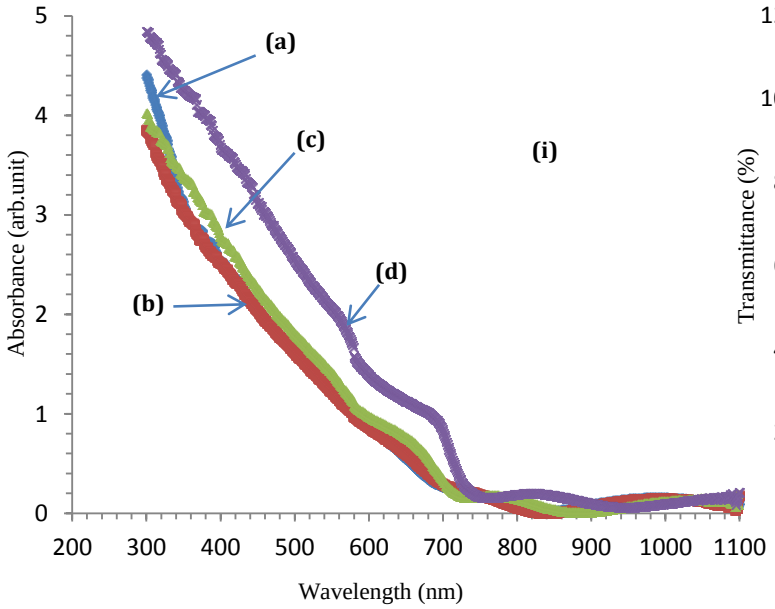

Fig. 4 (i). Plot of absorbance vs. wavelength for CdSe thin films (a) as-deposited, and annealed at (b) 473 K, (c) 573 K and (d) 673 K.

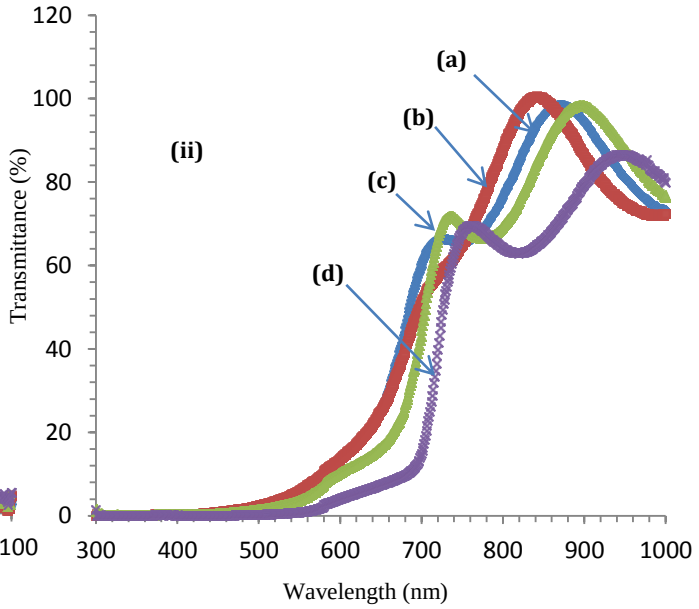

Fig. 4(ii) . Plot of transmittance vs. wavelength for CdSe thin films (a) as-deposited, and annealed at (b) 473 K, (c) 573 K and (d) 673 K.

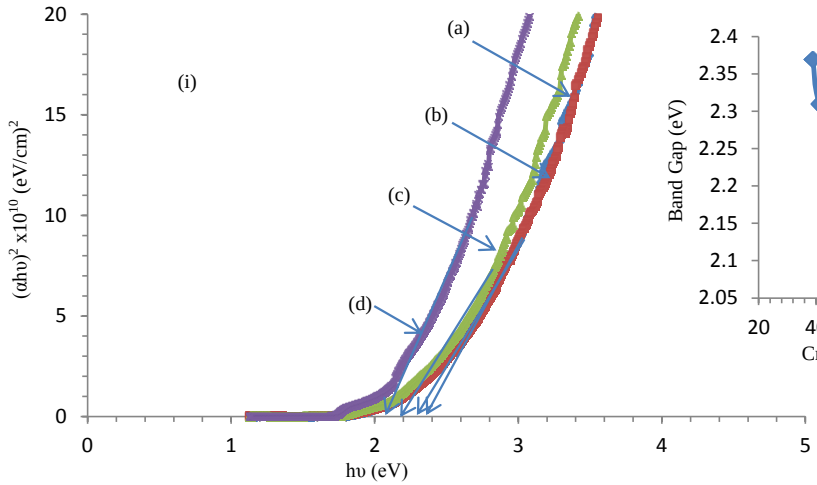

Fig. 5 (i). Plot of $(\alpha h\upsilon)^2$ vs. hυ for CdSe thin films (a) as-deposited, and annealed at (b) 473 K, (c) 573 K and (d) 673 K.

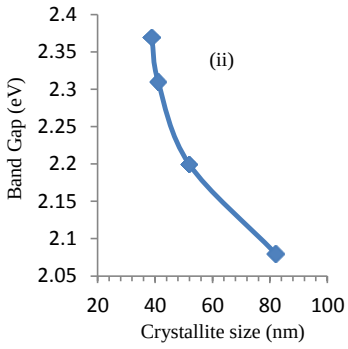

Fig. 5 (ii). Plot of band gap vs. grain size of CdSe thin films.

The refractive index (n) and dielectric constant (ε) of semiconducting materials are very important in determining the optical and electrical properties of the film which is essential for designing heterostructure lasers in optoelectronic devices as well as in solar cell applications. The refractive index is directly related to the fundamental energy band gap (E_g) by the Moss relation [40] equation (7)

$$E_g n^4 = k \qquad (7)$$

Where k is a constant with a value of 108 eV. A different relation between the refractive index and band gap energy is presented by Herve and Vandamme. The Herve and Vandamme [41] relation is given by the following equation (8)

$$n = \sqrt{1 + \left(\frac{A}{E_g + B}\right)^2} \quad (8)$$

Where A and B are numerical constants with values of 13.6 and 3.4 eV, respectively and the result is shown in Table 2. The dielectric behavior of solids is important for several electron-device properties. Both static and high frequency dielectric constants were evaluated for all the films. The high frequency dielectric constant (ε_∞) was calculated through the following relation equation (9)[40]

$$\varepsilon_\infty = n^2 \quad (9)$$

Where n is refractive index. The static dielectric constant (ε_0) [41] of the films was calculated using a relation expressing the energy band gap dependence of ε_0 for semiconductors compounds in the following form equation (10)

$$\varepsilon_0 = 18.52 - 3.08E_g \quad (10)$$

The calculated n, ε_∞ and ε_0 values of the CdSe films are presented in Table 2. Fig. 6 shows the variation in n and ε_∞ with energy band gap which calculated by using Moss relation and Herve & Vandamme relation.

3.3.Electrical properties

Electrical resistivity of CdSe film onto glass substrate was measured using a d.c. two point probe method in air in the temperature range from 300K to 430K. Figure 7 shows the variation of (Lnρ) with reciprocal of temperature (1/T)x10^3. It is observed that the resistivity decreases with increase of temperature, indicating semiconducting nature of films. The resistivity at room temperature was found to be of (2.55x10^3Ω.cm) of as-deposited CdSe thin films was decreased to (1.58x10^3Ω.cm) after annealing at temperature 673K. The high value of resistivity for as-deposited CdSe thin film may be attributed to the found some lattice defects, geometrical and physical imperfections randomly distributed on the surface and the volume of the film [42]. The roughness of the surface, grain boundaries and inclusions in the volume are the main components of the geometrical imperfection. The important factor, which is responsible for the physical properties of thin film, is the structure. An increase of temperature of the films affects the structure significantly causing a considerable increase in the mean size of the grain [43] and a decrease in the grain boundary area. This decrease is due to the migration of the smaller crystallites and joining of those grains, which are similarly oriented, to form bigger crystallites. Because of these structural changes the inter-grain boundary area decreases i.e. there is a decrease in the scattering of electrons. Consequently, the carrier concentration also increases with the increase of temperature. This in turn decreases the resistivity of given sample.

The thermal activation energy was calculated using the relation [44]:

$$\rho = \rho_o \, exp\left(\frac{E_o}{KT}\right) \quad (11)$$

Where, ρ is resistivity at temperature T, ρ_o is a constant, K is Boltzmann constant ($8.62x10^{-5}eV.K^{-1}$) and E_o is the activation energy required for conduction. Figure 8 shows variation in activation energy from 0.9935 to 0.0355 eV as annealing changes from 300 to 673 K. These observations may be due to size effects that are arising because of quantum confinement of charge carriers within the particles. Also the decrease in activation energy with annealing temperature is due to shifting of donor level towards conduction band. It suggests that the conduction in these thin films is due to the thermally assisted tunneling of the charge carriers through the grain boundary barrier and transition from donor level to conduction band [45].

Table 2. Crystalline size, band gap (Eg), refractive index, high frequency dielectric constant and static dielectric constant of as-deposited and annealed CdSe thin films.

Thin films	Crystalline size (nm)	Optical band gap "Eg" (eV)	Moss relation		Herve & Vandamme		ε_0
			n	ε_∞	n	ε_∞	
As-deposited	39	2.37	2.598	6.750	2.560	6.555	11.220
473 K	41	2.31	2.614	6.837	2.583	6.672	11.405
573 K	52	2.2	2.646	7.006	2.626	6.897	11.744
673 K	82	2.08	2.684	7.205	2.675	7.159	12.113

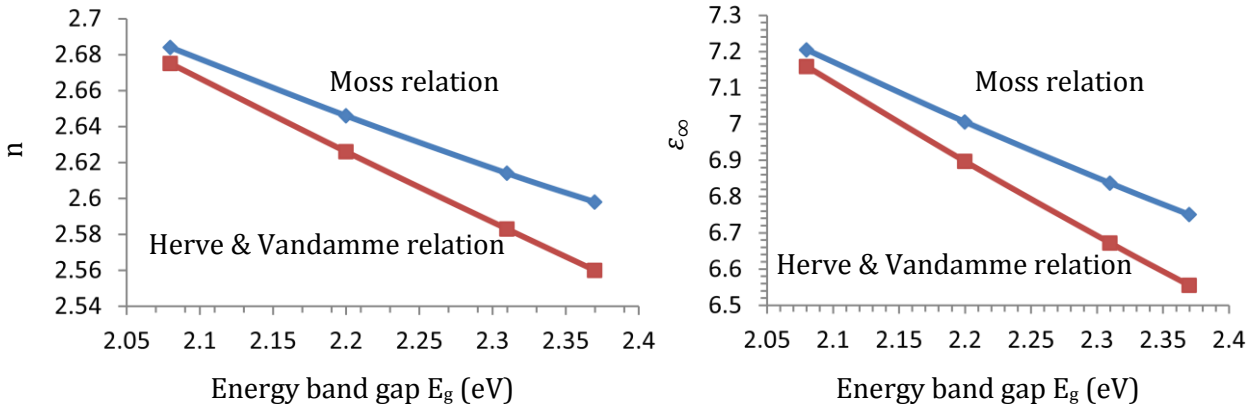

Fig. 6 Variation of n and ε_∞ with energy band gap of CdSe thin films.

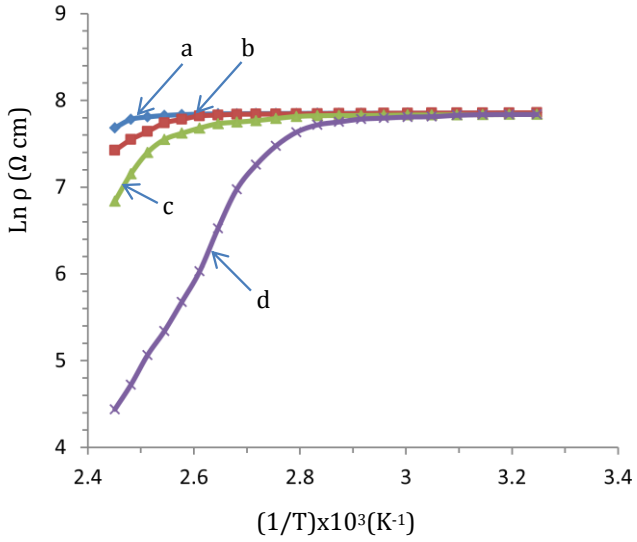

Fig. 7 Plot of Ln ρ vs. (1000/T) of CdSe thin films (a) as-deposited and annealed at (b) 473 K, (c) 573 K and (d) 673 K

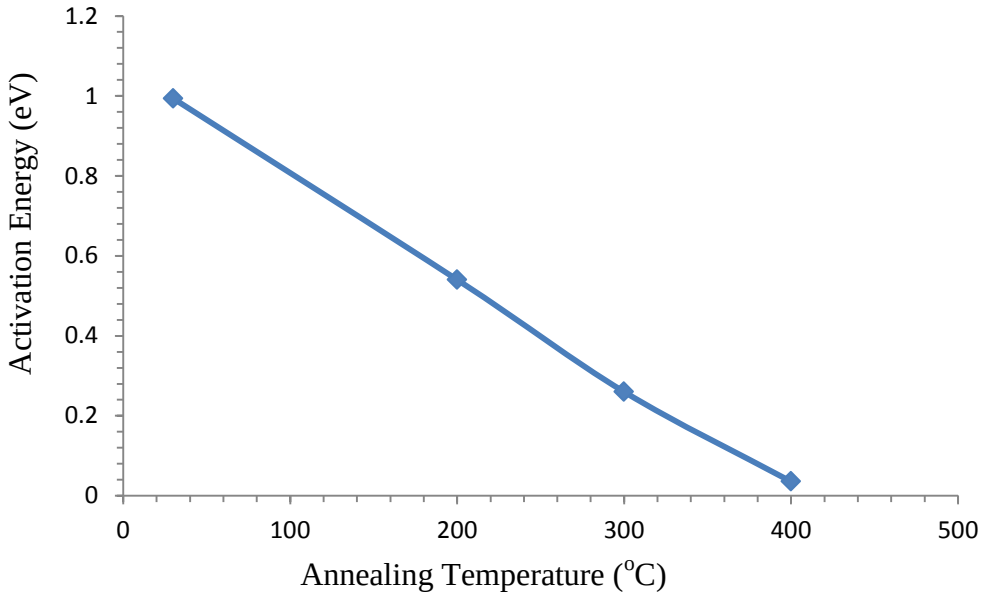

Fig. 8 Variation of activation energy of CdSe thin films with annealing temperature.

4. Conclusions

Polycrystalline CdSe thin films were successfully deposited on glass substrate at room temperature by thermal evaporation method. The prepared CdSe films were annealed in vacuum for 2h at 200°C, 300°C and 400°C and characterized for structural, optical and electrical properties. The structure of the films consists of fine and highly oriented grains with hexagonal (wurtzite) (002) planes. The crystalline nature of the film got enhanced due to increase in the crystallite size after annealing. The increase of optical absorption and decrease in transmittance with annealing temperature resulted in lowering of the band gap value which will be advantageous for its use in photovoltaic cells. The values of the optical band gap energy decreased from 2.37-2.08 eV with increased

the annealed temperature. The decrease of the electrical resistivity with the increase of annealing temperature is due to the increase of grain size and carrier density, then the electrical resistivity and therefore activation energy are observed to be temperature dependent.

References

1- Yiyang Gong, Nanomaterials for the Conversion of Solar Energy, Department of Electrical Enginering, Stanford University, Stanford, CA, 94305 March 17 (2009).

2- L. E. Brus, Appl. Phys. A 53 (1991) 465.

3- O. Millo, D. Katz, Y. W. Cao, U. Banin, Phys.Rev. Lett. 86 (2001) 5751.

4- Y. Wang, N. Heron, J. Phys. Chem. 95 (1991) 525.

5- A. Hengelein, Curr. Top. Chem. 143 (1998) 113.

6- T. Inokuma, T. Arai, M. Ishikawa, Phys. Rev. B **42** (1990) 1623.

7- N. N. Grrenwood, E. A. Earnshaw, Chemistry of the Elements, Oxford: Pergamon, London (1990),p.1403.

8- M. G. Bawendi, P. J. Carolli, W. L. Wilson, L. E. Brus, J. Phys. Chem. 96 (1992) 1335.

9- A. P. Alivisators, Science 271 (1996) 933.

10- L. W. Wang, A. Zunger, Phys. Rev. B 53 (1996) 9579.

11- J. M. Nedeljkovic, M. T. Nenadovic, O. I. Micic, A. J. Nozik, J. Phys. Chem. 90 (1986) 12.

12- H. Fujiwara, H. Hosokawa, K. Murakoshi, Y. Wada, S. Yanagida, T. Okada, H. Kobayashi, J. Phys. Chem. B 101 (1997) 8270.

13- S. Yanagida, M. Kanemoto, K. Ishihara, Y. Wada, T. Sakata, H. Mori, Bull. Chem. Soc. Jpn. 70 (1997) 2063.

14- R. Rossetti, S. Nakahara, L. E. Brus, J. Chem. Phys. 79 (1983) 1086.

15- W. Hoheisel, V. L. Colin, C. S. Johnson, A. P. Alivastos, J. Phys. Chem. 101 (1994) 5455.

16- Y. M. Niquet, G. Allan, C. Deleue, M. Lannoo, Appl. Phys. Lett. 77 (2000) 1182.

17- J. Nanda, B. A. Kuruvilla, K. V. P. Shafi, D. D. Sarma, in: K. P. Jain (Ed), Physics of Semiconducting Nanostructure, Narosa Publication, (1997), pp.25.

18- J. Nanda, B. A. Kuruvilla, D. D. Sarma, Phys. Rev. B 59 (1999) 7473.

19- A. L. Efros, m. Rosen, Ann. Rev. mater. Sci. 30 (2000) 475.

20- J. Jie, W. Zhang, I. Bello, Nano Today 5 (2010) 313-336.

21- M. C. Tamargo, "II-VI Semiconductor material and their application", Taylor and Francies, New York (USA) (2002).

22- E. U. Masumdar, and L. P. Deshmukh, Turk. J. Phys. **27**, 271-278 (2003).

23- Y. G. Gudage, N. G. Deshpande, A. A. Sagade, R. Sharma,n S. M. Pawar, C. H. Bhosale, Bell. Mater. Sci., **30** (4), 321-327 (2007).

24- Y. Zhao, Z. Yan, J. Liu and A. Wei, J. Materials Science in Semiconductor Processing, **16** (2013) 1592-1598.

25- Staff of Kaufman & Robinson, "The Ion Beam Authority," Technical Note KRI-06, pp. 1-2 (2006).

26- JCPDS Files No. 08-459 and 19-191.

27- JCPDS- International Centre for diffraction data, USA card No. 77-2307 (1998).

28- B.D. Cullity: Elements of X-ray diffraction (MA, Addison-Wesley Publishing Company, Boston 1978).

29- K. Sarmah, R. Sarma, H. L. Das, Chalc. Lett., **5**, 153 (2008).

30- G. K. Williamson and R. E. Smallman, Philos. Mag., **1**, 34 (1956).

31- SQ. Zhijie Wang, X. Zeng, C. Zhang, M. Shi, F. Tan, Z. Wang, et al., Polymer (2008), 49: 4647-51.

32- T. Dullweber, G. Hanna, U. Rau, HW. Schock, Solar Energy Materials & Solar Cells (2001), 67: 145-50.

33- T. S. Shyju, S. Anandhi, R. Indirajith, R. Gopalakrishnan, J. Crystal Growth, 337 (2011) 38-45.

34- R. Sivakumar, R. Gopalakrishnan, M. Jayachandran, C. Sanjeeviraja, Current Applied Physics **7** (2007) 51-59.

35- T. Mahalingam, A. Kathalingam, S. Velumani, L. Soonil, M. H. Sun, K. Y. Deak, Journal of Materials Science **41** (2006) 3553.

36- D.K. Dwivedi, V. Kumar, M. Dubey and H.P. Pathak, Chalcogenide Letters, **8**, 9, p.521-527(2011).

37- S.S. Kale and C.D. Lokhande, Mater. Chem. Phys. **62**, 103 (2000).

38- G. Hodes, A. Albu-Yaran, F. Decker and P. Matsuke, Phys. Rev. **B 36**, 476 (1962).

39- G. Hodes, Israel J. Chem. **33**, 95 (1993).

40- M.A. Yildirim, Optics Commun., 285, 1215-1220 (2012).

41- Rahul, S.R. Vishwakarma, R.N. Tripathi and A.K. Verma, Afr. Rev. Phys., 6,103-110 (2011).

42- K. C. Sharma and J. C. Gary, J. Phys. D: Appl. Phys. **23**, 1411 (1990).

43- C. Baran and G. I. Rusu, Appl. Surf. Sci. **211**, 6 (2003).

44- A. U. Ubale, A. R. Junghare, N. A. Wadibhasme, A. S. Daryapurakar, R. B. Mankar, and V. S. Sangawar, Turk J. Phys., 31, 279-286 (2007).

45- D. Patidar, N. S. Saxena and T. P. Sharma, J. Modern Optics **55**, 79 (2008).

الخواص التركيبية والضوئية والكهربائية المعتمدة على درجة حرارة التلدين للأغشية الرقيقة لمركب CdSe المرسبة حراريا

محمد محسن علي

قسم الفيزياء/ كلية العلوم / جامعة البصرة / البصرة ـ العراق

الخلاصة

تم ترسيب الاغشية الرقيقة للمركب CdSe على قواعد زجاجية بطريقة التبخير الحراري. وقد كان الضغط في حجرة التبخير ثابت عند المدى 10^{-6} الى 10^{-5} Torr على طول فترة الترسيب. ثم بعد ذلك تمت معاملة الأغشية الرقيقة حرارياً بالفراغ لمدة ساعتين بدرجات حرارية مختلفة ودراسة تأثير تلك المعاملة على مميزات الخواص التركيبية والضوئية والكهربائية. وقد تم تحديد التركيب البلوري ومعاملات الشبيكة للأغشية المحضرة والملدنة عن طريق تحليل حيود الاشعة السينية ولقد تبين ان الاغشية متناسقة وناعمة ومتعددة التبلور وتمتلك طوراً واحداً فقط وهو التركيب البلوري السداسي Hexagonal (wurtzite) وباتجاه نمو مفضل للمستوي (002) وبدون حدوث أي تغيير في التركيب البلوري خلال فترة التحضير وكذلك خلال عمليات التلدين. ولقد تم حساب الحجم البلوري وكثافات الانخلاع والاجهاد المايكروي بالنسبة للقمم التي تمتلك اعلى ارتفاع للأغشية المحضرة والملدنة. ولقد تم ملاحظة ان الحجم الحبيبي (الحجم البلوري) يزداد بينما تقل كثافات الانخلاع مع زيادة درجة حرارة التلدين. كذلك تمت دراسة أطياف الامتصاصية والنفاذية لتلك الاغشية باستخدام مطياف الحزمة المزدوجة UV-visible في مدى الاطوال الموجية 300-1100 nm ، ولقد حددت فجوات الطاقة باستخدام طيف الامتصاصية ولوحظ ان فجوات الطاقة تقل من 2.37 eV الى 2.08 eV مع زيادة درجة حرارة التلدين. وأيضاً تمت دراسة اعتماد فجوات الطاقة على الحجم البلوري، وحساب الممانعة الكهربائية وطاقة التنشيط للأغشية الرقيقة للمركب CdSe بطريقة Two Probe ومنها درست حالة نقصان الممانعة الكهربائية للتيار المستمر مع زيادة الحجم الحبيبي ايضاً.